Design of Experiments for Optimized Synthesis of Carbon-Supported Ni Nanoparticles: A Green Chemistry Approach

Axel Rigoulet, Thibault Rafaïdeen, Christophe Coutanceau, Têko W Napporn

ChemElectroChem

Research Article
doi.org/10.1002/celc.202400189

Chemistry Europe
European Chemical Societies Publishing

www.chemelectrochem.org

Design of Experiments for Optimized Synthesis of Carbon-Supported Ni Nanoparticles: A Green Chemistry Approach

Axel Rigoulet,[a] Thibault Rafaïdeen,[a] Christophe Coutanceau,*[a, b] and Têko W. Napporn*[a, b]

Metallic nickel nanoparticles supported on a high specific surface area carbon powder were synthesized by a classical polyol method without external reducing agent or surfactant. Ni/C materials were characterized by TGA, XRD, cyclic and linear voltammetry. To decrease the number of experiments, a Taguchi design of experiments (DoE) was implemented and the effects of different synthesis parameters (nature of the nickel salt, loading of Ni on carbon, n_{NaOH}/n_{Ni} ratio and reaction time at reflux) on different responses (crystallite size, electrochemically active surface area and current density for the glucose oxidation reaction at 1.5 V) determined. Optimization of parameter values for decreasing the crystallite size down to 14 nm was achieved using the DoE. For the other responses, strong interactions between parameters avoided straightforward optimization of parameter values. However, some trends could be drawn from the experimental matrix showing that the synthesis of a catalyst loaded with only 10 wt% Ni, with $NiCl_2$ as precursor salt, with a n_{NaOH}/n_{Ni} ratio of 6 for 80 minutes at reflux was a good compromise between atom, time and energy savings, costs efficiencies, and electrochemically active surface area and catalytic activity towards the glucose oxidation reaction, particularly in terms of mass activity.

Introduction

The increasing electrification of society based on intermittent renewable energy sources (wind, solar, tidal, etc.) requires the development of electrochemical energy storage and conversion technologies,[1,2] such as the electrochemical production of green hydrogen.[3] Hydrogen has indeed become an unavoidable molecule to achieve net zero carbon emission by 2050.[4]

Low-temperature alkaline water electrolyzer (AWE) and proton exchange membrane water electrolyzer (PEMWE) are the more mature systems[5] that have their own advantages and drawbacks.[5,6] The future development of anion exchange membrane water electrolysers (AEMWE) could combine the advantages of AWE and PEMFC and avoid part of their respective drawbacks.[5] But, the high stability of the water molecule involves high energy for its splitting into oxygen and hydrogen. The Gibbs energy corresponding to this reaction has a value of $+237\ kJ\,mol_{H_2}^{-1}$ at 25 °C and 0.1 MPa. This value leads to a reversible cell voltage of +1.229 V under these conditions, which corresponds to the minimum cell voltage needed to initiate the hydrogen and oxygen evolution reactions. As the oxygen evolution reaction (OER) is recognized as the limiting reaction in water electrolysis systems,[7–9] the electroreforming in alkaline media of biosourced organic compounds or wastes, such as alcohols, polyols, sugars, urea, etc., has received more and more attention.[10,11] Indeed, the thermodynamic data associated to the oxidation of oxygenated molecules[12] allow envisaging lower reversible cell voltages for their electrooxidation at the anode together with hydrogen production at the cathode of a biomass-assisted anion exchange membrane water electrolysis cell (biomass-assisted AEMWE).[13] Glucose is a good candidate for such an application: it can be produced from non-edible lignocellulosic biomass[14] and the reversible cell voltage involving the glucose oxidation reaction (GOR) at the anode and the hydrogen evolution reaction (HER) at the cathode is negative (−0.012 V).[12] For both systems, AEMWE and Biomass-assisted AEMWE, nickel-based nanoparticles (NPs) are considered as catalysts in both electrodes, anode for the OER[10,15,16] or for organic molecule oxidation reaction,[17–19] and cathode for the HER.[20–22] But nickel is also an important material for many others industrial applications, involving competition between them for this metal. For this reason, Nickel belongs to the list of strategical raw material of the European Commission owing to its importance for the green and digital transitions, and for defense and aerospace applications.[23] Therefore, the rationalization of its use in systems is of paramount importance.

Numerous synthesis methods have been developed for the preparation of nanostructured Ni-based materials. The reader can find their description in the reviews of Jaji et al.[24] and Kate et al.[25] for the synthesis of nickel and nickel oxide NPs, respectively. Tahmasebi et al.[26] used a water-in-oil microemulsion method for the synthesis of carbon-supported 3 nm spherical $Ni(OH)_2$ particles. To obtain metallic Ni particles, the synthesis methods often involve high temperature treatment. Jia et al.[27] prepared carbon supported Ni nanoparticles of ca.

[a] A. Rigoulet, Dr. T. Rafaïdeen, Prof. C. Coutanceau, Dr. T. W. Napporn
CNRS, Université de Poitiers Institut de Chimie des Milieux et Matériaux de Poitiers – IC2MP, Poitiers, France
E-mail: teko.napporn@univ-poitiers.fr
christophe.coutanceau@univ-poitiers.fr

[b] Prof. C. Coutanceau, Dr. T. W. Napporn
CNRS, French Research Network on Hydrogen (FRH2), Research Federation No. 2044 CNRS, France

Supporting information for this article is available on the WWW under https://doi.org/10.1002/celc.202400189

34.6 nm crystallite size by pyrolysis of nickel diamine–dicarboxylic acid metal organic frameworks (MOFs) at 800 °C in argon atmosphere. Recently, Fu et al.[28] used a Pechini-type sol-gel method for the preparation of supported Ni metal nanoparticles with crystallite size increasing from 6.9 to 23.5 nm when the temperature was increased from 400 to 650 °C. Visser et al.[29] deposited nickel on different carbon supports using incipient wetness impregnation followed by heat treatment under N_2 and N_2/H_2 atmospheres at 350 °C. They obtained mixtures of NiO and Ni metal phases, with crystallites size of ca. 5 nm.

The polyol route appears as a very versatile way to produce different metallic nickel structures at relatively low temperature, including NPs, particularly using ethylene glycol as reaction medium.[30] But although this synthesis method is very easy to implement, relatively few articles can be found on its use for the preparation of metallic nickel nanoparticles supported on a carbon support. Indeed, starting from nickel salts, it is relatively difficult to synthesize at low temperature metallic Ni-based spherical nanoparticles with size lower than several tenths of nm without adding surfactants or additional reducing agents in the reaction mixture, such as PVP[31,32] and hydrazine,[33] respectively. However, starting from a Ni acetate precursor, Okram et al.[34] showed that increasing the pH from 5.9 to 10.5 allowed decreasing the Ni particle size from ca. 40 to ca. 13 nm.

In the present contribution, a classical polyol method was used for the synthesis of carbon supported metallic Ni nanoparticles from different nickel salts, without addition of any additive in ethylene glycol, except sodium hydroxide. Since the final microstructure of the Ni NPs, their electrochemically active surface area and their activity towards the GOR depend on the synthesis parameters, a coherent method, i.e. a design of experiments (DoE), was implemented to reduce the number of experiments implied by the number of parameters studied (here, nature of the Ni salt precursor, targeted theoretical metal loading, n_{NaOH}/n_{Ni} molar ratio and time at reflux) and to rationalize the interpretation of the results. The objective was also to propose a synthesis method allowing decreasing the mean Ni crystallite size (atom economy), and increasing electrochemically active surface area (EASA) and activity of catalysts towards the GOR (improved efficiency). Therefore, such approach enters completely the scope of the green chemistry principles.[35]

Table 1. values assigned for each parameter at each level.

	Level 1	Level 2	Level 3
Ni salt	$NiCl_2 \cdot 6\ H_2O$	$Ni(Ac)_2 \cdot 4\ H_2O$	$Ni(NO_3) \cdot 6\ H_2O$
Ni (mmol)	53.7	113.4	255.1
n_{NaOH}/n_{Ni}	3	6	9
t @ T_r (min)	40	80	120

Table 2. L_9 (3^4) orthogonal array of Taguchi. A, B, C and D are the studied parameters with their level for the corresponding experiment.

Experiments	Parmeters			
	A	B	C	D
Exp. 1	1	1	1	1
Exp. 2	1	2	2	2
Exp. 3	1	3	3	3
Exp. 4	2	1	2	3
Exp. 5	2	2	3	1
Exp. 6	2	3	1	2
Exp. 7	3	1	3	2
Exp. 8	3	2	1	3
Exp. 9	3	3	2	1

Results and Discussion

Implementation of the DoE

For the optimization of the polyol synthesis of metallic Ni NPs, 4 parameters are considered, each set at 3 different values (levels). This corresponds to a full factorial design of experiments involving 81 experiments (3^4).[36,37] This large number of experiments involves three important consequences: it is very consuming in terms of atoms, energy, time, and therefore very costly, the 81 results for each considered response will make difficult their unequivocal interpretation and finally the optimization will be impossible to perform.

The very convenient mathematical and statistical Taguchi method can allow reducing the number of experiments, while keeping an acceptable accuracy in the interpretation of

Table 3. Matrix of experiments and measured responses: experimental crystallite size $L_{v(exp.)}$, "nominal" $ECSA_{(exp.)}$ from nominal Ni loadings, "actual" $ECSA_{(exp.)}$ from actual Ni loadings determined by TGA (Table 5), and experimental geometric current density $j_{(exp.)}$ @ 1.5 V.

Parameters Experiments	Ni salt	Ni wt.%	$\frac{n_{NaOH}}{n_{Ni}}$	t @ t_r min	$L_{v(exp.)}$ /nm	"Nominal" $ECSA_{(exp.)}$ $/m^2\ g_{Ni\ nominal}^{-1}$	"Actual" $ECSA_{(exp.)}$ $/m^2\ g_{Ni\ actual}^{-1}$	$j_{(exp.)}$ @ 1.5 V /mA cm^{-2}
Exp. 1	$NiCl_2$	5	3	40	15.8	83.8	72,3	3.0
Exp. 2	$NiCl_2$	10	6	80	36.5	116.0	154,6	4.9
Exp. 3	$NiCl_2$	20	9	120	40.0	58.4	57,3	4.9
Exp. 4	$Ni(Ac)_2$	5	6	120	21.8	69.9	81,3	2.6
Exp. 5	$Ni(Ac)_2$	10	9	40	43.3	79.8	57,4	4.6
Exp. 6	$Ni(Ac)_2$	20	3	80	37.3	72.0	50,7	5.3
Exp. 7	$Ni(NO_3)_2$	5	9	80	23.4	69.8	60,1	2.9
Exp. 8	$Ni(NO_3)_2$	10	3	120	28.8	89.8	98,7	4.7
Exp. 9	$Ni(NO_3)_2$	20	6	40	36.4	75.2	75,2	4.8
Average					31.5	79.4	78,6	4.2

results.[37] Such a method has already been successively employed for optimizing carbon supported Pt-based catalysts.[38,39] However, since the standard redox potential of Ni^{2+} to metallic Ni ($E^\circ = -0.257$ V vs SHE) is much lower than that of Pt^{2+} to metallic Pt ($E^\circ = +1.2$ V vs SHE), the formation of small metallic nickel nanoparticles without any additional reducing agent and/or surfactant, through direct reduction of Ni^{2+} atoms by intermediates from EG oxidation[40] is much more difficult, which also justifies the need to optimize the synthesis procedure. Indeed, the difference in redox potential of metal salts involves different reaction mechanisms (as explained in the review of Fievet et al.[40]) and therefore different influent parameters. Table 1 gives the values assigned for each parameter at each level. As we only want to obtain an optimization of the system (possible interactions between parameters are neglected), the model we consider is very simple:

$$Y_i = \bar{R} + E_{s,i} + E_{W,i} + E_{r,i} + E_{t,i} \quad (1)$$

where, Y_i is the theoretical response of the system for the experience (i), $\bar{R}$ the response's average of all experiments in the DoE, and $E_{s,i}$, $E_{w,i}$, $E_{r,i}$ and $E_{t,i}$ are the mean effects of the Ni^{2+} salt nature, of the theoretical Ni loading (wt%), of the n_{NaOH}/n_{Ni} molar ratio and of the reaction time at the reflux temperature (t @ T_r), respectively, at the considered level i in experiment.

The number of degrees of freedom of the system is 9 (1 for the average and two for each effect) and at least 9 experiments must be done to respect the condition of orthogonality of the fractional DoE (each parameter appearing the same number of times at a given level). Therefore, the number of experiments can be decreased from 81 down to 9 using the basic L_9 (3^4) orthogonal array of Taguchi (Table 2).

From the L_9 (3^4) orthogonal array, the experimental matrix has been constructed, and the responses determined for each experiment (Table 3). The mean effects of each parameter on each response can be calculated using equation 2 (for parameter A as an example), and further discussed.

$$E_{A_i} = \frac{\sum R_{A_i}}{3} - \bar{R} \quad (2)$$

where E_{Ai} is the effect of parameter A at the level i, R_{Ai} are the measured responses for parameter A at the level i and $\bar{R}$ the response's average of all experiments.

Table 4 reports the values of the effects calculated from Table 3 and Equation (2). From the values of the effects, it should be possible to determine the best configuration of the parameters and to optimize the responses of the system in terms of crystallite size (L_v), electrochemically active surface area (EASA) and activity for the GOR (j @ 1.5 V).

Table 4. Values of the effects (Es, Ew, Er, and Et) for their different levels calculated from experimental results in Table 3 and equation (2).

	Ni salt (E_s)	Ni wt% (E_w)	$\frac{n_{NaOH}}{n_{Ni}}$ (E_r)	t @ t_r (E_t)
L_v (nm)				
Level 1	−0.710	−11.144	−4.178	0,355
Level 2	2.655	4.722	0.089	0,922
Level 3	−1.945	6.422	4.089	−1,277
ECSA ($m^2 g_{Ni\ nominal}^{-1}$)				
Level 1	6.668	−4.924	2.465	0.210
Level 2	−5.501	15.784	7.601	6.495
Level 3	−1.167	−10.861	−10.066	−6.705
ECSA ($m^2 g_{Ni\ actual}^{-1}$)				
Level 1	16.111	−7.389	−4.722	−10,322
Level 2	−15.489	24.944	25,078	9.844
Level 3	−0.622	−17.556	−20.356	0,478
j @ 1.5 V (mA cm^{-2})				
Level 1	0.08	−1.352	0.143	−0.051
Level 2	−0.03	0.532	−0.080	0.153
Level 3	−0.05	0.820	−0.063	−0.102

Physicochemical Characterization of Electrocatalysts

Different carbon support can be used for the deposition of metal catalysts.[41] Amongst these supports, Vulcan XC 72 possesses physicochemical properties that made it a standard support for electrocatalysts. Vulcan XC72 has particles size of ca. 50–60 nm diameter (Figure 1), a specific surface area of ca. 250 $m^2 g^{-1}$, a total pore volume of 0.63 $cm^3 g^{-1}$, mainly mesoporous (microporous pore volume being only 3.7×10^{-2} $cm^3 g^{-1}$), and a conductivity of 5.3 S cm^{-1}.[42]

The catalysts are first analyzed by TGA in order to assess their actual metal loadings. Table 5 displays the value determined from thermograms given in supporting information, SI 1. For Ni/C catalysts prepared with $NiCl_2$ and $Ni(NO_3)_2$ precursor salts, the experimental loadings are close to the nominal ones. The catalysts prepared with the $Ni(Ac)_2$ salt display higher loading values than the nominal ones, which can be due to the presence of remaining acetate salts. Indeed, XRD patterns showed the presence of diffraction peaks assigned to acetate salts (supporting information, SI 3), likely sodium acetate as NaOH is a reactant in the polyol synthesis procedure. TEM

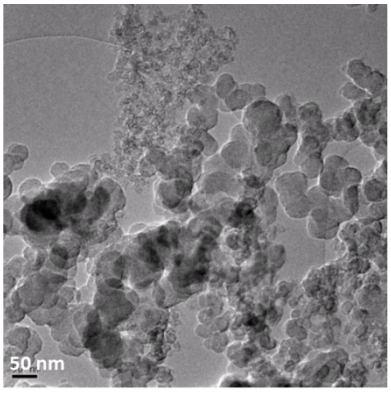

Figure 1. TEM image of the Vulcan XC72 carbon support.

Table 5. Values of the metal loadings for the different catalysts prepared from the experimental conditions in the design of experiments.

Nominal Ni loading	5 wt%			10 wt%			20 wt%		
Ni salt	$NiCl_2$	$Ni(AC)_2$	$Ni(NO_3)_2$	$NiCl_2$	$Ni(AC)_2$	$Ni(NO_3)_2$	$NiCl_2$	$Ni(AC)_2$	$Ni(NO_3)_2$
Actual Ni Loading	5.8 wt%	4.3 wt%	5.8 wt%	7.5 wt%	13.9 wt%	9.1 wt%	20.4 wt%	28.4 wt%	20.0 wt%

images were also recorded to have an idea of the particle sizes and morphology of the catalysts. However, different Ni structures were obtained, from spherical small nanoparticles to shaped particles of several tenths of nm (Supporting information, SI 2), which makes the determination and comparison of particle size irrelevant, as well as the comparison of catalytic activity on this basis.

Therefore, the first response considered in the DoE is the crystallite size represented by the Scherrer length, L_v, and determined from the most intense peak of Ni NPs in XRD patterns recorded on each catalyst (supporting information, SI 3) using the Scherrer equation:[43]

$$L_v = \phi \frac{\lambda}{\mathrm{FWHM}\cos\theta} \quad (3)$$

with ϕ the shape factor (0.89 for spherical crystallite), λ the radiation wavelength (1.5406 Å), FWHM the full width at half-maximum, and θ the angle at the maximum intensity.

Figure 2 displays exemplary XRD patterns of three Ni NPs/C electrocatalysts prepared from experiments 1, 2 and 3 of the DoE. The other XRD patterns are given in supporting information, SI 3. The peak deconvolution for each diffraction pattern was performed using a pseudo-Voigt function in the Highscore Plus software. The XRD patterns for the carbon-supported Ni NPs display diffraction peaks at $2\theta = 44.5°$, 51.9°, 76.4°, 92.9° and 98.4°, confirming the formation of metallic Ni in a face centered cubic (fcc) structure (JCPDS file no. 4-0850). The diffraction peak at $2\theta = 24.8°$ corresponds to the graphite crystallites of the carbon support.[44] It should be noted that all the catalysts prepared for this work display the metallic cfc structure of Ni and that no diffraction peak corresponding to $Ni(OH)_2$ or NiO is observed (supporting information, SI 3). Other diffraction peaks are present for 2θ lower than 60° in the case of the catalysts prepared from $Ni(ac)_2$ salt, which are likely due to remaining sodium acetate salt after rinsing.

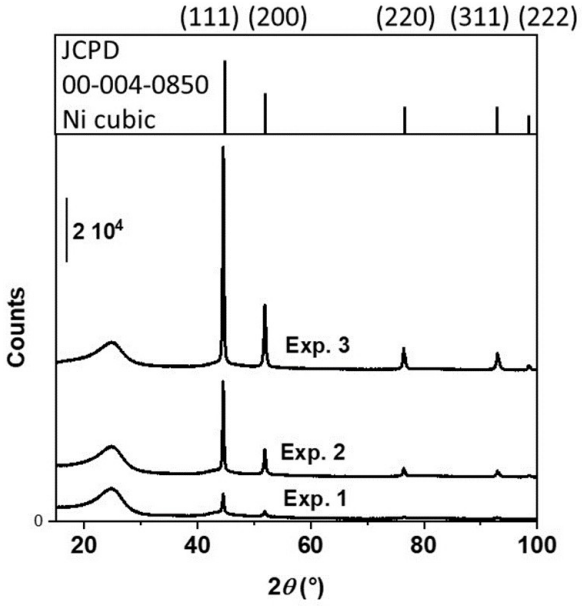

Figure 2. XRD patterns of carbon-supported Ni NPs/C catalysts synthesized with different configurations of parameters. The peak "C" corresponds to the graphite of the carbon support.

The first remark is that the most influencing parameters on the L_v value are the Ni weight loading on carbon and the ratio n_{NaOH}/n_{Ni}. Carroll et al.[45] studied the $NiCl_2$ (Ni^{2+}) salt reduction into Ni^0 during the polyol synthesis and showed that the mechanism involved the formation of Ni alkoxides complexes ($Ni^{2+}(CH_2OH–CH_2O^-)_2$). Scheme 1 shows the reaction mechanism for Ni reduction into Ni metal. Takahashi et al.[46] showed in the case of $CoCl_2$ reduction during a polyol synthesis method that the formation of the $Co^{2+}(CH_2OH–CH_2O^-)_2$ complexes occurred even in weak alkaline medium. In the same time, high concentrations of OH^- can favor the formation of $Ni(OH)_2$,[47] at the expense of the generation of $Ni^{2+}(CH_2OH–CH_2O^-)_2$ complexes, decreasing the nucleation site density for Ni particles. Therefore, decreasing the OH^- concentration with respect to Ni^{2+} concentration will lead to lower the formation of $Ni(OH)_2$ species and to increase that of $Ni(EG^-)_2$ complexes that act as nucleation sites for Ni crystallites, and furthermore will allow decreasing the crystallite size.

The best configuration of parameters for this response is E_s level 3, E_w level 1, E_r level 1 and E_t level 3. This configuration of parameters is out of the DoE (Table 2), and will further serve as a confirmation experiment (Exp. 10). From this configuration,

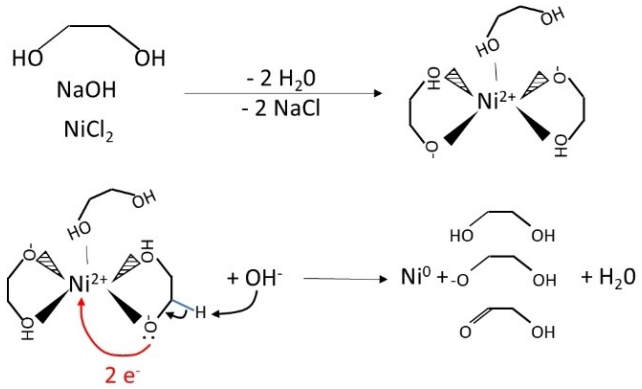

Scheme 1. mechanism for the reduction of $NiCl_2$ to Ni-metal during the polyol synrhesis method, as proposed by Caroll et al..[45]

and using equation (1), the theoretical L_v value is calculated to ca. 13 nm, whereas the experimental value determined from the XRD pattern (Exp. 10 in supporting information, SI 3) of the Ni NPs is ca. 16 nm. Although this value is twice lower than the average value of L_v (31.5 nm) obtained from the DoE, which is already a very good result according to the objective, it is slightly higher than the theoretical one, and this difference can be due to the standard deviation of measurements or to the existence of interactions between parameters.

It is worth to note that the second better configuration of parameters (E_s level 1, E_w level 1, E_r level 1 and E_t level 3), also out of the DoE (Exp. 11), leads to the same theoretical and experimental L_v values of ca. 14 nm (Exp. 11 in supporting information, SI 2). This indicates that the influence of interactions between parameters, if existing, is very small for this response.

Electrochemical Evaluation of Electrocatalysts

Figure 3 compares exemplary the typical stable CVs recorded in N_2-purged 0.1 M NaOH/1.0 M Na_2SO_4 electrolyte at 20 mV s^{-1} on the three catalysts prepared from $Ni(NO_3)_2$ salt precursor (Exps. 7, 8 and 9 of the DoE). The other CVs can be accessed in supporting information, SI 4. Although XRD measurements indicated that metallic Ni particles were obtained using the polyol method, the CVs are typical of those for β-$Ni(OH)_2$ electrodes in alkaline medium, with the β-$Ni(OH)_2$/β-NiOOH redox transition in the 1.1 to 1.5 V vs RHE potential range.[31] Indeed, the reversible $Ni(OH)_2$/Ni redox couple can only be observed when cycling in a potential range from ca. −0.2 V to 0.5 V vs RHE. As soon as the electrode is cycled in higher potential region, an irreversible β-$Ni(OH)_2$ structure forms at the surface of the electrode.[48] Catalysts obtained with the different metal salt precursors lead to the same electrochemical behavior: a shift of the Ni^{2+} to Ni^{3+} redox peaks towards lower potentials and increase of the oxidation and reduction peak current density with the increase of the Ni weight loading. The EASA of the Ni NPs/C catalysts was determined by integrating, after correction of the double layer capacitive current, the reduction current density in the NiOOH to $Ni(OH)_2$ reduction peak between 1.425 V and 1.200 V, and considering a charge of 420 μC cm^2 for the reduction of a monolayer of NiOOH into $Ni(OH)_2$.[49] The EASA values calculated from the nominal Ni weight loadings and from the actual Ni weight loadings determined by TGA are given in Table 3 for all catalysts in the DoE. From these results, the effects of the different parameters were calculated (Table 4), and the best configuration of parameters was E_s level 1, E_w level 2, E_r level 2 and E_t level 2 for both the "nominal" and "actual" EASAs. This configuration of parameters leading to the highest theoretical and experimental EASA values of 116 $m^2 g_{Ni}^{-1}$ (nominal) and 154.6 $m^2 g_{Ni}^{-1}$ (actual) belongs to the DoE.

The electrocatalytic activity towards the GOR of the Ni NPs/C catalysts has been evaluated by recording LSVs from 1.0 V to 1.55 V in N_2-purged 0.1 M NaOH/1.0 M Na_2SO_4 containing 0.1 M glucose at 20 mV s^{-1}. For sake of clarity, Figure 4 presents only the LSVs for catalysts prepared from Exp. 1, Exp. 2 and Exp. 3 of the DoE as examples. The other LSVs are accessible in supporting information, SI 5. It has been reported that the catalytic activity is driven by the redox potential of the Ni^{2+}/Ni^{3+} transition,[50] so that the onset potential of the glucose electrooxidation reaction is relatively high, e.g. 1.2 V vs RHE. The mechanism has been proposed to proceed through an electrochemical/chemical catalytic process (EC′) involving the $Ni(OH)_2$ surface oxidation into NiOOH that reacts with organic oxygenated species to form intermediates/products while being reduced into $Ni(OH)_2$.[51,52]

The current density achieved at 1.5 V is chosen as the descriptor of the activity. Results are given in Table 3. From the mean value of j @ 1.5 V (Table 3) and the determination of the effects (Table 4), the best configuration of parameters seems to be E_s level 1, E_w level 3, E_r level 1 and E_t level 2, leading to the highest theoretical value for j @ 1.5 V of 5.4 mA cm^{-2}. This

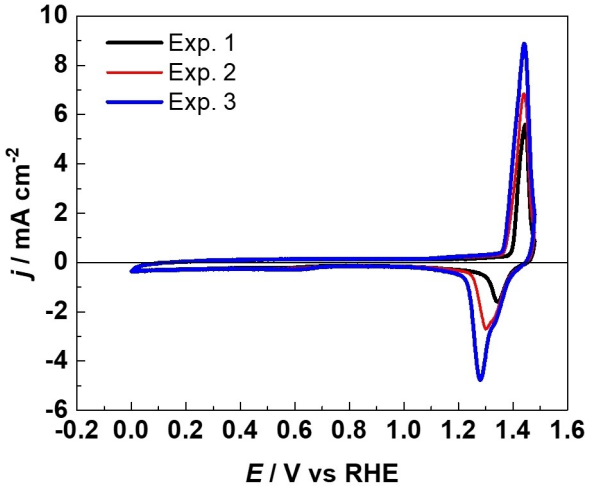

Figure 3. Cyclic voltammograms of carbon-supported Ni NPs/C catalysts synthesized with different configurations of parameters recorded in N_2-purged 0.1 M NaOH/1.0 M Na_2SO_4 supporting electrolyte (scan rate = 20 mV s^{-1}, T = 25 °C).

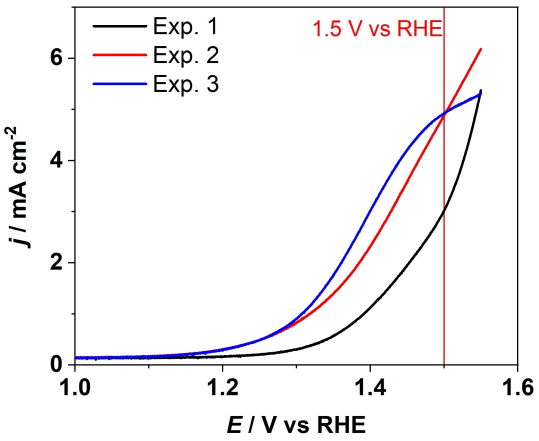

Figure 4. Linear scan voltammograms of carbon-supported Ni NPs/C catalysts synthesized with different configurations of parameters recorded for the oxidation of 0.1 M glucose in N_2-purged 0.1 M NaOH/1.0 M Na_2SO_4 supporting electrolyte (scan rate = 20 mV s^{-1}, T = 25 °C).

configuration is out of the DoE (Exp. 12) and has been used, as well as the two other configurations out of DoE configurations (Exp. 10 and Exp. 11) for L_v, as confirmation experiment for both EASA and *j* @ 1.5 V responses. Results are given in Table 6.

If the theoretical and experimental values for the crystallite size are very close for all confirmation experiments, indicating that the DoE is accurate for this response, this is not the case for the EASA and *j* @ 1.5 V responses. The experimental values are always lower than the theoretical ones. For these two responses it seems that strong interactions between parameters must be considered, and then determined. The consideration of only one interaction between parameters will lead to increase the number of experiments to 27, and to 81 (full factorial design of experiments) if 2 or more independent interactions are considered. Such situation will be atom, time, energy and money consuming, and not compatible with industrial development.

However, some trends can be drawn from the confirmation experiments and the experimental matrix. First, the experimental values of EASA and mass activity (MA expressed in mA/mg_{Ni}) @ 1.5 V decrease with the increase of the nickel loading and of the crystallite size, whereas experimental *j* and surface activity (SA expressed in mA/cm_{Ni}^{2}) @ 1.5 V increases. This behavior suggests that a compromise has to be found. According to the results in Table 3, catalysts loaded with 10 wt% Ni give about the same current density at 1.5 V as those loaded with 20 wt% (close to 5 $mA\,cm^{-2}$), indicating that their MA is almost twice higher, while those loaded at 5 wt% give a current density value almost twice lower. This can be explained considering that under the present experimental conditions, the mechanism of glucose electrooxidation is not only limited by its diffusion towards NiOOH active sites but also by its adsorption on $Ni(OH)_2$ sites. Indeed, Mandrano-Banda et al.[53] proposed recently that glucose electrooxidation on $Ni(OH)_2$/NiOOH catalysts followed a dual path involving an Eley-Rideal mechanism on NiOOH species (diffusion limited) and a Langmuir-Hinshelwood mechanism between adsorbed glucose on $Ni(OH)_2$ species and NiOOH (adsorption limited). Therefore, the catalysts prepared from $NiCl_2$, with loading of 10 wt%, at 80 °C for 80 minutes at T_r represents a very good compromise between atom, energy and time savings, and EASA and activity for the GOR.

Conclusions

A design of experiments derived from a Taguchi $L_9(3^4)$ orthogonal array has been implemented to try to improve the polyol synthesis of carbon supported Ni nanoparticles in terms of lower mean crystallite sizes (L_v), and higher EASA and activity towards the GOR at 1.5 V. The implementation of the DoE allowed reducing the number of experiments from 81 for the full factorial design to 9 for the fractional one, saving atoms, time, energy and money. The decrease of the Scherrer length down to 14 nm could be achieved thanks to the optimization of the synthesis parameter levels proposed by the study, because possible interactions between parameters were negligible. However, smaller crystallite sizes were obtained for lower Ni loadings, which in turn led to lower activity towards the GOR.

In terms of EASA and activity towards the GOR, strong interactions between synthesis parameters exist, and optimizations are not straightforward. However, the analysis of the experimental matrix (Table 3) clearly indicates that the activity towards the GOR at 1.5 V is almost the same for catalysts loaded with 10 wt% Ni as for those loaded with 20 wt%, Ni, i.e. with twice less catalytic material. The synthesis in Exp. 2, starting from $NiCl_2$ as precursor salt, targeting a Ni loading of 10 wt%, with n_{NaOH}/n_{Ni} molar ratio of 6 and *t* @ T_r of 80 minutes, is an excellent compromise since it allows obtaining a catalyst with very high EASA (116 $m^2\,g_{Ni}^{-1}$) and *j* @ 1.5 V (4.9 $mA\,cm^{-2}$), while minimizing the amount of Ni and NaOH used (atom saving), as well as the temperature and reaction time (energy saving).

From a more general point of view, the present study also shows that design of experiments are very powerful methods not only to optimize systems, but also to reduce the number of experiments to do this. Therefore, they could play an important role in the implementation of green chemistry approaches.

Experimental Section

Materials

Nickel chloride ($NiCl_2 \cdot 6\ H_2O$, purum p.a., ≥ 98 %), nickel nitrate ($Ni(NO_3) \cdot 6\ H_2O$, assay spec., ≥ 98.5 %), nickel acetate ($Ni(Ac)_2 \cdot 4\ H_2O$, ≥ 99.995 %), sodium hydroxide (NaOH, reagent grade, ≥ 98 %), sodium sulfate (Na_2SO_4, ACS reagent, ≥ 99 %), ethylene glycol (EG, reagent plus, ≥ 99 %) and Nafion® suspension (5 wt.% in aliphatic

Table 6. Values of the metal loadings for the different catalysts prepared from the experimental conditions in the design of experiments.

		Exp. 10	Exp. 11	Exp. 12
L_v/nm	Theo	12.9	14.2	33.9
	Exp	15.8	14	36.5
EASA/$m^2\,g_{Ni}^{-1}$	Theo	69.1	76.6	84.2
	Exp	95.3	62.9	21
j@1.5 V/mA cm_{geom}^{-2}	Theo	2.87	2.96	5.4
	Exp	2.0	1.6	3.5
SA@1.5 V/mA cm_{Ni}^{-2}	Exp	0.17	0.20	0.33
MA@1.5 V/mA mg_{Ni}^{-1}	Exp	163	129	70

alcohols) were purchased from Sigma-Aldrich. The carbon powder (Vulcan XC72) from Cabot corp.

Synthesis of Catalysts

Mixtures of x mmol Ni salt in 10 mL EG and of y mmol NaOH in 5 mL EG were first prepared. In a three neck-flask, 59.9 mg of carbon support (previously heat-treated 4 hours at 400 °C under N_2 atmosphere to remove impurities) were mixed under magnetic stirring to 10 mL EG. A solution of Ni salt was added in the three-neck flask and let to mix for several minutes under stirring. Then a solution of NaOH was added in the three-neck flask and let to mix under magnetic stirring. After 10 minutes mixing, the mixture was heated at reflux (temperature T_r) and maintained at this temperature for z h (t @ T_r). At the end of the synthesis procedure, the mixture was allowed to cool down to room temperature, then filtrated over a 0.22 μm hydrophilic PVDF membrane filter (Durapore® from Millipore) and washed several times with acetone and ultrapure water (MilliQ from Millipore, 18.2 MΩ cm resistivity). The retentate was dried overnight in an oven at 60 °C. Table 1 gives the three different values for each of the four synthesis parameters, which were used in this contribution.

Characterization of Catalysts

The protocol of characterization of catalyst is described elsewhere.[54] Thermogravimetric analysis TGA (TGA, TA Instrument model SDT Q 600) was used to assess their actual metal loading, x-ray diffraction (XRD, PANalytical Empyrean X-ray diffractometer) to determine their crystallite size (Scherrer length), scanning electron microspcopy - energy dispersive x-ray (SEM-EDX, SEM FEG JSM-7900F Jeol) to evaluate repartition of Ni NPs on the support and catalytic powder composition.

Electrochemical Evaluation of Catalysts

The catalytic ink is prepared by mixing 10 mg of a catalytic powder with 1.495 mL of ultrapure water and 0.175 μL of the Nafion suspension. The mixture is homogenized by ultrasonication for 30 min (Fisherbrand 15051 ultrasonic bath, 2.75 L, 37 kH, 320 W). The working electrode is prepared by dispensing 8.3 μL of the ink on a 5 mm diameter glassy carbon disc previously mirror-polished (A3 γ-Al_2O_3 paste, A1 γ-Al_2O_3 paste, and ultrasonication). The ink drop is uniformized and dried under 400 rpm rotation and N_2 flow.

The electrochemical set-up was composed of an interfaced PGZ 100 Voltalab (Radiometer Analytical) potentiostat and a three-electrode thermostated electrochemical cell fitted with a 3 cm^2 glassy carbon (GC) as counter-electrode, a reversible hydrogen electrode (RHE, HydroFlex from Gaskatel) as refence and the 0.5 mm diameter working electrode. Cyclic voltammograms (CVs) and linear scan voltammograms (LSVs) were recorded in N_2-purged 0.1 M NaOH /1.0 M Na_2SO_4 supporting electrolyte in the absence or in the presence 0.1 M glucose, respectively, at $T = 25$ °C and with a potential scan rate of 20 mV s^{-1}. All potentials are quoted to the reversible hydrogen electrode. The protocols of electrode activation until stable CVs and LSVs are explained in supporting information, SI 6.

Acknowledgements

The authors thank the European Union's Horizon Europe research and innovation program under grant agreement No 101070856 ELOBIO for funding, as well as the European Union (ERDF), the Région Nouvelle Aquitaine and the INCREASE research federation (FR CNRS 3707) for supports. This work pertains to the French government program "Investissements d'Avenir" (EUR INTREE, reference ANR-18-EURE-0010). AR also thanks M. Weliton Silva Fonseca for fruitful scientific discussions.

Conflict of Interests

The authors declare no conflict of interest.

Data Availability Statement

The data that support the findings of this study are openly available in Zenodo at https://zenodo.org/doi/10.5281/zenodo.10697403.

Keywords: Design of Experiments · Electrooxidation · Glucose · Metallic nickel · Synthesis

[1] S. P. S. Badwal, S. S. Giddey, C. Munnings, A. I. Bhatt, A. F. Hollenkamp, *Front. Chem.* **2015**, *2*, 79.
[2] M. Carmo, D. Stolten, in *Science and engineering of hydrogen-based energy technologies: hydrogen production and practical applications in energy generation* (Ed.: P. E. V. de Miranda), Elsevier BV Amsterdam, **2019**, pp. 165–199.
[3] International Energy Agency, "A Roadmap for the Global Energy Sector" can be found under https://www.iea.org/reports/net-zero-by-2050, **2021** (accessed October 24th, 3023).
[4] International Energy Agency, "Global Hydrogen Review 2021" can be found under https://www.iea.org/reports/global-hydrogen-review-2021, **2021** (accessed October 24th, 2023).
[5] M. Chatenet, B. G. Pollet, D. R. Dekel, F. Dionigi, J. Deseure, P. Millet, R. D. Braatz, M. Z. Bazant, M. Eikerling, I. Staffell, P. Balcombe, Y. Shao-Horn, H. Schäfer, *Chem. Soc. Rev.* **2022**, *51*, 4583.
[6] C. Coutanceau, S. Baranton, T. Audichon, *Hydrogen Electrochemical Production, in Hydrogen Energy and Fuel Cells Primers*, (Ed.: B. G. Pollet), Elsevier, Amsterdam, **2018**. Pp. 59–62.
[7] C. Lamy, T. Jaubert, S. Baranton, C. Coutanceau, *J. Power Sources* **2014**, *245*, 927.
[8] Z. Chen, X. Duan, W. Wei, S. Wang, B.-J. Ni, *Nano Energy* **2020**, *78*, 105392.
[9] E. K. Volk, S. Kwon, S. M. Alia, *J. Electrochem. Soc.* **2023**, *170*, 064506.
[10] C. Dollé, N. Neha, C. Coutanceau, *Curr. Opin. Electrochem.* **2022**, *31*, 100841.
[11] V. M. Zemtsova, A. G. Oshchepkov, E. R. Savinova, *ACS Catal.* **2023**, *13*, 13466.
[12] C. Lamy, C. Coutanceau, S. Baranton, *Production of clean hydrogen by the electrochemical reforming of oxygenated organic compounds, In Hydrogen and Fuel cells primers.* (Ed.: B. G. Pollet), Elsevier, Amsterdam, **2020**, pp. 9–12.
[13] M. Yang, Z. Yuan, R. Peng, S. Wang, Y. Zou, *Energy Environ. Mater.* **2022**, *5*, 1117.
[14] T. Rafaïdeen, S. Baranton, C. Coutanceau, *ChemElectroChem* **2022**, *9*, e202101575.
[15] L.-A. Stern, X. Hu, *Faraday Discuss.* **2014**, *176*, 363.
[16] L. Trotochaud, S. L. Young, J. K. Ranney, S. W. Boettcher, *J. Am. Chem. Soc.* **2014**, *136*, 6744.
[17] M. S. E. Houache, R. Safari, U. O. Nwabarac, T. Rafaïdeen, G. A. Botton, P. J. A. Kenis, S. Baranton, C. Coutanceau, E. A. Baranova, *ACS Appl. Energ. Mater.* **2020**, *3*, 8725.
[18] A. G. Oshchepkov, G. Braesch, A. Bonnefont, E. R. Savinova, M. Chatenet, *ACS Catal.* **2020**, *10*, 7043.

[19] M. E. Ghaith, M. G. Abd El-Moghny, G. A. El-Nagar, H. H. Alalawy, M. E. El-Shakre, M. S. El-Deab, *Electrochim. Acta* **2023**, *452*, 142325.
[20] Z. Liang, H. S. Ahn, A. J. A. Bard, *J. Am. Chem. Soc.* **2017**, *139*, 4854.
[21] A. Y. Faid, A. O. Barnett, F. Seland, S. Sunde, *J. Electrochem. Soc.* **2019**, *166*, F519.
[22] F. Foroughi, M. Tintor, Al. Y. Faid, S. Sunde, G. Jerkiewicz, C. Coutanceau, B. G. Pollet, *ACS Appl. Energ. Mater.* **2023**, *6*, 520.
[23] M. Grohol, C. Veeh, European Commission, Directorate-General for Internal Market, Industry, Entrepreneurship and SMEs, "Study on the critical raw materials for the EU 2023 – Final report", Publications Office of the European Union (2023), https://data.europa.eu/doi/10.2873/725585.
[24] N.-D. Jaji, H. L. Lee, M. H. Hussin, H. Md Akil, M. R. Zakaria, M. B. H. Othman, *Nanotechnol. Rev.* **2020**, *9*, 1456.
[25] R. S. Kate, S. A. Khalate, R. J. Deokate, *J. Alloys Compd.* **2018**, *734*, 89.
[26] S. Tahmasebi, S. Jahangiri, N. Mosey, G. Jerkiewicz, A. Mark, S. Cheng, G. Botton, S. Baranton, C. Coutanceau, *ACS Appl. Energ. Mater.* **2020**, *3*, 7294.
[27] M. Jia, C. Choi, T.-S. Wu, C. Ma, P. Kang, H. Tao, Q. Fan, S. Hong, S. Liu, Y.-L. Soo, *Chem. Sci.* **2018**, *9*, 8775.
[28] Y. Fu, F. Devred, P. Eloy, T. Haynes, M. L. Singleton, S. Hermans, Y. Jung, J. Qiua, Z. Sun, *Appl. Catal. A* **2022**, *644*, 118833.
[29] N. L. Visser, J. C. Verschoor, L. C. J. Smulders, F. Mattarozzi, D. J. Morgan, J. D. Meeldijk, J. E. S. van der Hoeven, J. A. Stewart, B. D. Vandegehuchte, P. E. de Jongh, *Catal. Today* **2023**, *418*, 114071.
[30] F. Fiévet, S. Ammar-Merah, R. Brayner, F. Chau, M. Giraud, F. Mammeri, J. Peron, J.-Y. Piquemal, L. Sicarda, G. Viau, *Chem. Soc. Rev.* **2018**, *47*, 5187.
[31] X. Liu, K. Huang, S. Zhou, P. Zhao, U. Meridor, A. Frydman, A. Gedanken, *J. Magn. Magn. Mater.* **2006**, *305*, 504.
[32] G. G. Couto, J. J. Klein, W. H. Schreiner, D. H. Mosca, A. J. de Oliveira, A. J. Zarbin, *J. Colloid Interface Sci.* **2007**, *311*, 461.
[33] S.-H. Wu, D.-H. Chen, *J. Colloid Interface Sci.* **2003**, *259*, 282.
[34] G. S. Okram, A. Soni, R. Prasad, *Adv. Science Lett.* **2011**, *4*, 132.
[35] P. Anastas, N. Eghbali, *Chem. Soc. Rev.* **2010**, *39*, 301.
[36] P. Schimmerling, J. C. Sisson, A. Zaïdi, *Pratique des plans d'expériences*, Lavoisier Tec & Doc, Paris, **1998**.
[37] R. K. Roy, *A primer on the Taguchi method*, Society of Manufacturing Engineers, Dearborn, Michigan, Second Edition, **2010**.
[38] C. Grolleau, C. Coutanceau, F. Pierre, J. M. Leger, *J. Power Sources* **2010**, *195*, 1569.
[39] E. Lebègue, S. Baranton, C. Coutanceau, *J. Power Sources* **2011**, *196*, 920.
[40] F. Fiévet, S. Ammar-Merah, R. Brayner, F. Chau, M. Giraud, F. Mammeri, J. Peron, J.-Y. Piquemal, L. Sicard, G. Viau, *Chem. Soc. Rev.* **2018**, *47*, 5187.
[41] E. Antolini, *Appl. Catal. B* **2009**, *88*,1.
[42] F. Maillard, P. Simonov, E. R. Savinova, in *Carbon Materials for Catalysis*, Vol. 5, (Eds. P. Serp, J. L. Figueiredo), John Wiley & Sons, Inc, New York, **2009**, pp. 429–480.
[43] B. E. Warren, *X-Ray Diffraction*, Dover Publications, NewYork, **1990**.
[44] H. Zhu, X. Li, F. Han, Z. Dong, G. Yuan, G. Ma, A. Westwood, K. He, *Carbon* **2016**, *99*, 174.
[45] K. J. Carroll, J. U. Reveles, M. D. Shultz, S. N. Khanna, E. E. Carpenter, *J. Phys. Chem. C* **2011**, *115*, 2656.
[46] K. Takahashi, S. Yokoyama, T. Matsumoto, J. L. Cuya Huaman, H. Kaneko, J.-Y. Piquemal, H. Miyamura, J. Balachandran, *New J. Chem.* **2016**,*40*, 8632.
[47] K. Yu, D. J. Kim, H. S. Chung, H. Liang, *Matter. Lett.* **2003**, *57*, 3992.
[48] D. S. Hall, C. Bock, B. R. MacDougall, *J. Electrochem. Soc.* **2013**, *160*, F235.
[49] E. Cossar, M. S. E. Houache, Z. Zhang, E. A. Baranova, *J. Electroanal. Chem.* **2020**, *870*, 114246.
[50] C. Coutanceau, S. Baranton, R. S. B. Kouamé, *Front. Chem.* **2019**, *7*, 100.
[51] M. Fleischmann, K. Korinek, D. Pletcher, *J. Electroanal. Chem.* **1971**, *31* 39.
[52] M. Fleischmann, K. Korinek, D. Pletcher, *J. Chem. Soc.-Perkin Trans.* **1972**, *2*, 1396.
[53] A. Medrano-Banda, J. Guehl, G. Kéranguéven, A. Oshchepkov, E. Savinova, A. Bonnefont, *Electrochim. Acta* **2024**, *476*, 143692.
[54] S. Baranton, C. Coutanceau, *Appl. Catal. B* **2013**, *136–137*, 1.

Manuscript received: February 26, 2024
Revised manuscript received: March 23, 2024
Version of record online: ■■, ■■

RESEARCH ARTICLE

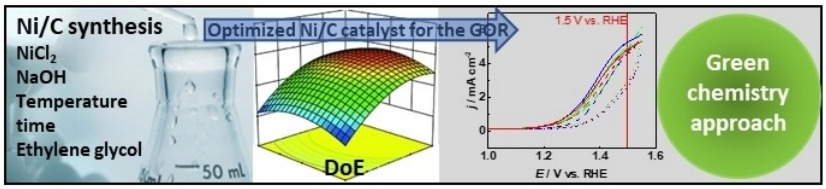

Implementation of a Design of Experiments is a very powerful mean to optimize with a minimum of experiments the polyol synthesis of metallic nickel catalysts active towards glucose electrooxidation reaction. Here, a low metal loaded catalyst, prepared with minimum amounts of reactants (Ni and NaOH), and a minimum reaction time at reflux, led to achieving the highest activity. By allowing saving atoms, time, energy and therefore money, such a tool clearly belongs to the green chemistry approaches.

A. Rigoulet, Dr. T. Rafaïdeen, Prof. C. Coutanceau, Dr. T. W. Napporn**